

# Factors affecting phase synchronization in integrate-and-fire oscillators

Todd W. Troyer

Received: 24 May 2005 / Revised: 9 November 2005 / Accepted: 11 November 2005 / Published online: 22 April 2006  
© Springer Science + Business Media, LLC 2006

**Abstract** Step changes in input current are known to induce partial phase synchrony in ensembles of leaky integrate-and-fire neurons operating in the oscillatory or “regular firing” regime. An analysis of this phenomenon in the absence of noise is presented based on the probability flux within an ensemble of generalized integrate-and-fire neurons. It is shown that the induction of phase synchrony by a step input can be determined by calculating the ratio of the voltage densities obtained from fully desynchronized ensembles firing at the pre and post-step firing rates. In the limit of low noise and in the absence of phase synchrony, the probability density as a function of voltage is inversely proportional to the time derivative along the voltage trajectory. It follows that the magnitude of phase synchronization depends on the degree to which a change in input leads to a uniform multiplication of the voltage derivative over the range from reset to spike threshold. This analysis is used to investigate several factors affecting phase synchronization including high firing rates, inputs modeled as conductances rather than currents, perithreshold sodium currents, and spike-triggered potassium currents. Finally, we show that without noise, the equilibrium ensemble density is proportional to the phase response curve commonly used to analyze oscillatory systems.

**Keywords** Exponential integrate-and-fire · Phase response curve · Population density · Synchrony

## Introduction

It is well-known that transient changes in inputs can cause populations of leaky integrate-and-fire (LIF) oscillators to partially synchronize their spiking output (Brown et al., 2004a; Gerstner, 2000; Knight et al., 2000), and that patterns of synchrony in a neuron’s input can play an important role in determining its output (Salinas and Sejnowski, 2001). Thus, understanding the biophysical mechanisms that control this synchronization can play an important role in uncovering the functional properties of neural circuits (e.g. Brown et al., 2004b).

The phenomenon of transient-induced phase synchronization is clearly illustrated by considering the firing rate of a large ensemble of identical LIF neurons driven by a fixed external current. In the low-noise or “regular firing” regime, each LIF neuron acts like a neural oscillator, producing a regular train of action potentials. The ensemble firing rate is defined as the density of spikes produced at any given time, and is directly analogous to the peri-stimulus time histogram (PSTH) commonly measured in electrophysiological experiments (Fig. 1). Assuming that the ensemble is completely desynchronized, the ensemble rate will be constant and equal to the reciprocal of the interspike interval (ISI) in an individual neuron, termed the “ISI rate.” If the external current undergoes a step increase, two things happen: (i) the overall ensemble rate also undergoes a step increase; (ii) the ensemble rate oscillates with a period equal to the ISI of individual neurons (Fig. 1, left). This oscillation reflects partial phase synchronization: all neurons in the ensemble have a identical ISIs, but more neurons are firing at some phases of the oscillation than at others.

The usual explanation for this phenomenon is that the leak current causes the voltage trajectory to slow down as

---

Action Editor: John Rinzel

T. W. Troyer (✉)  
Department of Psychology, University of Maryland,  
College Park, MD 20742  
e-mail: ttroyer@glue.umd.edu

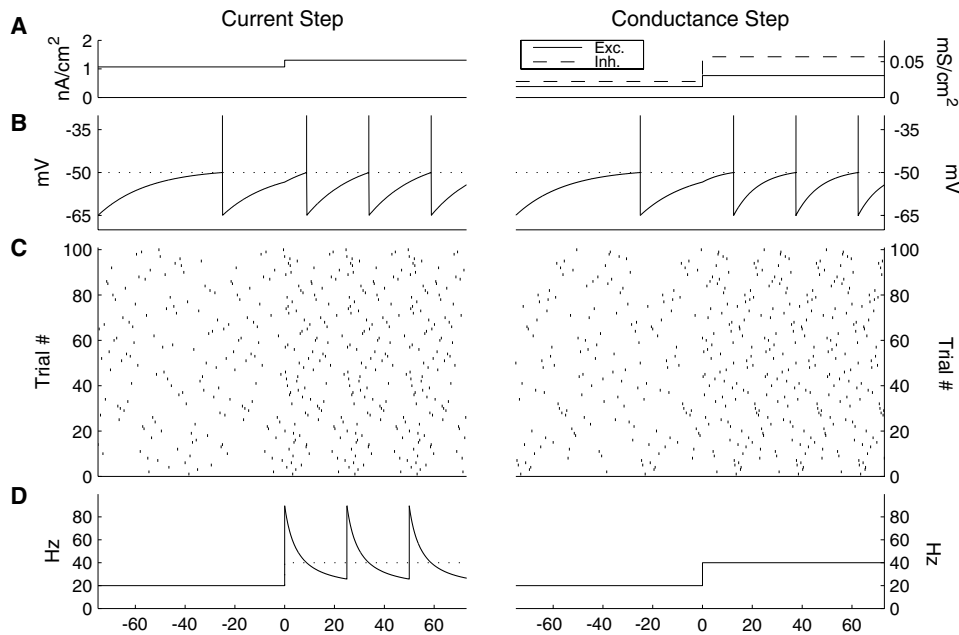


**Fig. 1** Partial phase synchronization may or may not result from step changes in input. (A) A step change in input is introduced to the LIF model at time  $t = 0$  producing a change in rate from 20 to 40 Hz in individual neurons (see section Mechanisms Affecting Phase Synchronization for parameters). Left: step increase in current ( $1.067 \rightarrow 1.301 \mu\text{A}/\text{cm}^2$ ). Right: step increase in excitatory and inhibitory conductances (ex:  $0.0152 \rightarrow 0.0305 \text{ mS}/\text{cm}^2$ ; inh:  $0.0223 \rightarrow 0.0570 \text{ mS}/\text{cm}^2$ ). (B) Example voltage traces starting with  $V = V_{\text{reset}}$  at  $t = -75$  msec. (C) Raster plot of  $n = 100$  trials with equally spaced initial phases shown

in randomized order. (D) Analytically calculated ensemble firing rate, analogous to the PSTH from a raster plot with  $n \rightarrow \infty$ . The step change in current induces partial phase synchrony, resulting in an oscillation of the ensemble firing rate. For conductance-step plots (right), the leak conductance was reduced and pre-step synaptic inputs were chosen so that the total conductance matched that of the current-based simulations before the step. Specific values of the input conductances were chosen in order to eliminate phase synchrony (see Fig. 3 legend for parameters)

it nears threshold. Taking a snap-shot of the distribution of voltages, an excess fraction will have voltages just below threshold. When the current is increased, these neurons will cross threshold together resulting in a transient increase in the ensemble rate above and beyond the step increase in the ISI rate. Although this explanation is largely correct, it is incomplete. This becomes clear if we consider a change in rate due to a sudden change in synaptic conductance, rather than a step change in input current. For specific patterns of conductance change, the ensemble can display sudden changes in firing rate yet remain completely desynchronized (Fig. 1, right; see section on Synaptic Conductances in Results). In both cases, before the transition there is an excess fraction of the ensemble having voltages just below threshold. But for the conductance change, this excess fraction does not give rise to phase synchronization.

This article aims to clarify the factors contributing to phase synchronization within a broad class of generalized integrate-and-fire (IF) models. A simple framework for understanding this phenomenon is derived based on the well-known population density approach (e.g. Fourcaud-Trocme and Brunel, 2005; Gerstner and Kistler, 2002; Knight, 1972; Moreno-Bote and Parga, 2005; Naundorf et al., 2005; Nykamp and Tranchina, 2000). This framework is then used to examine how several biological mechanisms affect phase

synchrony. In particular, we show how differences in overall spike rates, peri-threshold sodium currents, after-spike potassium currents, and synaptic conductances affect the magnitude of transient-induced phase synchronization.

## Methods

We confine most of our analyses to the class of generalized IF neurons whose subthreshold dynamics is defined by

$$C \frac{dV}{dt} = F(V) + I \quad (1)$$

where  $C$  is the membrane capacitance,  $F(V)$  is the total intrinsic membrane current, and  $I$  an external or synaptic current. For the standard LIF model,  $F(V) = g_l(V_{\text{rest}} - V)$  where  $g_l$  is the leak conductance and  $V_{\text{rest}}$  is the resting potential. Recently researchers have considered additional nonlinear terms. Two popular models are the quadratic integrate-and-fire model (Ermentrout, 1996; Latham et al., 2000) and the exponential integrate-and-fire (EIF) model (Fourcaud-Trocme et al., 2003), named for the functional form of a nonlinear term added to the leak current. The “fire” aspect of these models is implemented by marking a spike whenever

the voltage trajectory reaches a fixed value of the voltage  $V_{\text{spike}}$ , resetting the voltage to a value  $V_{\text{reset}}$ , and then returning to Eq. (1). A defining feature of this class of models is their one dimensional nature. The resetting property serves to dynamically “connect” the spiking and reset voltages, effectively turning voltage into a circular variable (Ermentrout and Kopell, 1986). If the input current is large enough, the voltage derivative is always positive and the neuron oscillates, tracing repeated circles around its one-dimensional state space.

All simulations included a step change in input current from a level  $I^-$  before the step to  $I^+$  after the step. Currents were chosen by using firing frequency vs. current (f–I) curves to determine the levels of current needed to produce specified single unit firing rates on either side of the step,  $r^-$  and  $r^+$ . Values for the one dimensional LIF model were generated analytically. For the EIF model, f–I curves were generated via numerical simulations with constant current stepped at  $0.001 \mu\text{A}/\text{cm}^2$  intervals. Linear interpolation of the f–I values was used to determine the level of current level needed to produce a given rate. Theoretically, the spiking voltage for the EIF model is set to be  $V_{\text{spike}} = +\infty$ . Practically, at depolarized voltages the exponential current completely dominates the dynamics, and the time that it takes for the voltage to diverge to infinity can be calculated analytically using this current alone. Following Fourcaud-Trocme et al. (2003), we let  $V_{\text{spike}} = -30 \text{ mV}$  and set spike times 0.066 msec later. Simulations used the Euler method with  $dt = 0.001 \text{ msec}$  and linear interpolation to more accurately determine the time at which voltage crossed  $V_{\text{spike}}$ . For both models, post-transition ensemble rates were determined analytically according to Eq. (10) derived below.

We also considered a two-dimensional LIF model with an added spike-triggered potassium conductance:

$$C \frac{dV}{dt} = F(V) + u(V_K - V) + I \tag{2}$$

$$\tau_u \dot{u} = -u \tag{3}$$

$$u \rightarrow u_{\text{reset}} \text{ after a spike} \tag{4}$$

where  $V_K$  is the potassium reversal potential. Levels of current injection were determined using simulated f–I curves as above. The dynamics of the exponentially decaying potassium conductance was solved analytically, whereas the voltage trajectory was determined using Euler’s method. To determine post-transition ensemble firing rates in this model, numerical simulations of 201 trajectories were performed. Their initial conditions delimited 200 intervals (size = .25 msec) that were equally spaced before the input step. The ensemble rate after the step was estimated as the inverse of the corresponding interspike intervals.

## Results

### Population densities

To analyze the dynamics of the ensemble firing rate, we use the population density approach. This approach has a long history in computational neuroscience (e.g. Amari, 1974; Knight, 1972; Stein, 1965; Wilson and Cowan, 1972), and has been exploited and elaborated by a number of researchers over the past several years (e.g. Brunel, 2000; Fourcaud-Trocme and Brunel, 2005; Gerstner and Kistler, 2002; Moreno-Bote and Parga, 2005; Naundorf et al., 2005; Nykamp and Tranchina, 2000; Omurtag et al., 2000). We consider an ensemble of solutions to the IF model given by Eq. (1), and examine the dynamics of the density of solutions as a function of time and voltage. That is, we want to examine the dynamics of the density function  $\rho(t, V)$  where  $\rho(t, V) dV$  is the probability of finding a given solution in a small interval of width  $dV$  around the voltage  $V$  at time  $t$ . To keep things simple, we will consider noiseless systems with piecewise constant inputs. The addition of low levels of noise yields similar dynamics but with an additional diffusive term that pushes the voltage distribution toward equilibrium. High levels of noise can drive the dynamics into the “random firing” regime where the model no longer acts like an oscillator.

Our analysis is directed toward formalizing the intuition that in the LIF model there is an “excess” of solutions near threshold that causes a surge of firing when the current is suddenly increased. Consider an initial density  $\rho_0(V)$ . If  $\rho_0(V)$  is large at a certain value of  $V$ , this will result in a high firing rate after a delay equal to the time it takes for solutions starting at  $V$  to reach threshold. Similarly a small value of  $\rho_0(V)$  will result in a low firing rate after an appropriate delay. To define “large” and “small” relative to the appropriate baseline, we assume that the ensemble begins in the fully desynchronized state where the density of phases (not of voltages) is uniform. In this state, the rate at which trajectories “flow past” any voltage  $V$  will be independent of  $V$  (and time). This flow rate is known as the probability flux, and for noiseless systems is equal to the density of solutions at a given voltage,  $\rho(V)$ , multiplied by their velocity,  $\frac{dV}{dt}(V)$ .

The ensemble firing rate  $r$  is simply the flow rate (flux) crossing the spiking voltage.

$$r = \rho(V_{\text{thresh}}) \frac{dV}{dt}(V_{\text{thresh}}) \tag{5}$$

For the desynchronized state,  $r$  is constant and equal to the ISI rate  $r_{\text{ISI}}$ . Since the flux is independent of voltage,

$$r_{\text{ISI}} = \tilde{\rho}(V) \frac{dV}{dt}(V) \tag{6}$$

$$\tilde{\rho}(V) = \frac{r_{\text{ISI}}}{\frac{dV}{dt}(V)} \tag{7}$$

where  $\tilde{\rho}(V)$  denotes the density in the desynchronized state. Thus, for noiseless systems *the equilibrium density is inversely proportional to the voltage derivative* (Ricciardi, 1977).

By definition, if the initial density  $\rho_0(V) = \tilde{\rho}(V)$  then the ensemble fires at a constant rate. However, suppose that the initial density  $\rho_0(V_0)$  were twice as large as equilibrium density  $\tilde{\rho}(V_0)$  for some initial voltage  $V_0$ . This increased density will flow toward threshold and eventually result in a firing rate equal to two times  $r_{\text{ISI}}$ <sup>1</sup>. More generally, the density  $\tilde{\rho}(V_0)$  forms the appropriate baseline so that the ratio  $\rho_0(V_0)/\tilde{\rho}(V_0)$  determines whether the initial density results in an increased or decreased firing rate when reaching threshold. That is,

$$r(t) = r_{\text{ISI}} \frac{\rho_0(V_0(t))}{\tilde{\rho}(V_0(t))} \tag{8}$$

where  $V_0(t)$  is the initial voltage of the trajectory that produces a spike at time  $t$ .

Equation (8) yields a simple method for analytically calculating the ensemble firing rate after a step change in input at time  $t = 0$ . We will use  $+/-$  superscripts to denote quantities related to the system after/before the change in input. Suppose that the ensemble is desynchronized for  $t < 0$  with density  $\tilde{\rho}^-(V)$ . Given a sudden change at  $t = 0$ , this density serves as the initial condition for the dynamics with  $t > 0$ . Letting  $\tilde{\rho}^+(V)$  be the desynchronized density for the level of input after the step, we have

$$r(t) = r_{\text{ISI}}^+ \frac{\tilde{\rho}^-(V_0(t))}{\tilde{\rho}^+(V_0(t))} \tag{9}$$

where  $r_{\text{ISI}}^+$  is the ISI rate after the step. So for step inputs, the pattern of phase synchrony is determined by the ratio of the desynchronized densities before and after the step. Now we can use Eq. (7) to write the firing rate in terms of the voltage derivative:

$$r(t) = r_{\text{ISI}}^+ \frac{r_{\text{ISI}}^- / \frac{dV}{dt}^-(V_0(t))}{r_{\text{ISI}}^+ / \frac{dV}{dt}^+(V_0(t))} = r_{\text{ISI}}^- \frac{\frac{dV}{dt}^+(V_0(t))}{\frac{dV}{dt}^-(V_0(t))} \tag{10}$$

If we denote the ratio of voltage derivatives before and after the step change in input by  $\alpha(V)$ , we have

$$r(t) = r_{\text{ISI}}^- \alpha(V_0(t)) \tag{11}$$

<sup>1</sup> The presentation here is related to the method of characteristics for solving partial differential equations.

It follows that *the magnitude of phase synchronization is determined by the degree to which changes in input lead to a uniform multiplication of the voltage derivative along the path from  $V_{\text{reset}}$  to  $V_{\text{spike}}$ .*

### Mechanisms affecting phase synchronization

To illustrate how various biological mechanisms affect the range of  $\alpha$  values, and hence phase synchronization, we consider a step change in input that increases single unit firing rates from  $r_{\text{ISI}}^- = 20$  Hz to  $r_{\text{ISI}}^+ = 40$  Hz. Although not discussed, the effects of step decreases in input can be readily understood by inverting the arguments presented below. As a particular example, we start with a typical LIF model:  $F(V) = g_l(V_{\text{rest}} - V)$ , with  $C = 1 \mu\text{F}/\text{cm}^2$ ,  $R = 1/g_l = 20 \text{ m}\Omega/\text{cm}^2$ ,  $V_{\text{rest}} = -70$  mV,  $V_{\text{spike}} = -50$  mV, and  $V_{\text{reset}} = -65$  mV. We find that the maximum and minimum firing rates after a step increase in external current are 89.8 Hz and 25.7 Hz respectively, corresponding to  $\alpha = 4.49$  and  $\alpha = 1.29$  (Fig. 1D, left). The remainder of this section explores several mechanisms affecting phase synchronization. For conceptual simplicity, we describe our results in terms of the conditions necessary to reduce phase synchronization from the relatively high levels of synchronization seen in this model.

### Firing rate effects

If we take the identical LIF model and consider a step change in current that doubles the ISI rate from 100 to 200 Hz instead of from 20 to 40 Hz, transient-induced synchronization is reduced. The maximum and minimum firing rates after the step are 229 Hz and 178 Hz respectively, corresponding to  $\alpha = 2.49$  and  $\alpha = 1.78$ . The reason why the phase synchronization is reduced at high rates can be understood in several ways (cf. Brown et al., 2004b; Hermann and Gerstner, 2001). Intuitively, at high rates the voltage doesn't slow down much as it approaches spike threshold. As a result, there is no surplus of solutions sitting just below threshold that spike as a group when rates are increased. Analytically, the equation for  $\alpha(V)$  is

$$\alpha(V) = \frac{\frac{dV}{dt}^+(V)}{\frac{dV}{dt}^-(V)} = \frac{F(V) + I^+}{F(V) + I^-} \tag{12}$$

where  $I^-$  and  $I^+$  represent the levels of current before and after the step. It follows that if the external currents  $I^+$  and  $I^-$  are significantly larger than the intrinsic currents  $F(V)$ , then  $\frac{dV}{dt}^+ / \frac{dV}{dt}^- \approx I^+ / I^-$  for all  $V$ . Since  $\alpha(V)$  is nearly constant, the phase synchrony induced by the transient change from  $I^-$  to  $I^+$  will be small. Graphically, at higher rates the range of voltage derivatives rests on top of a relatively high

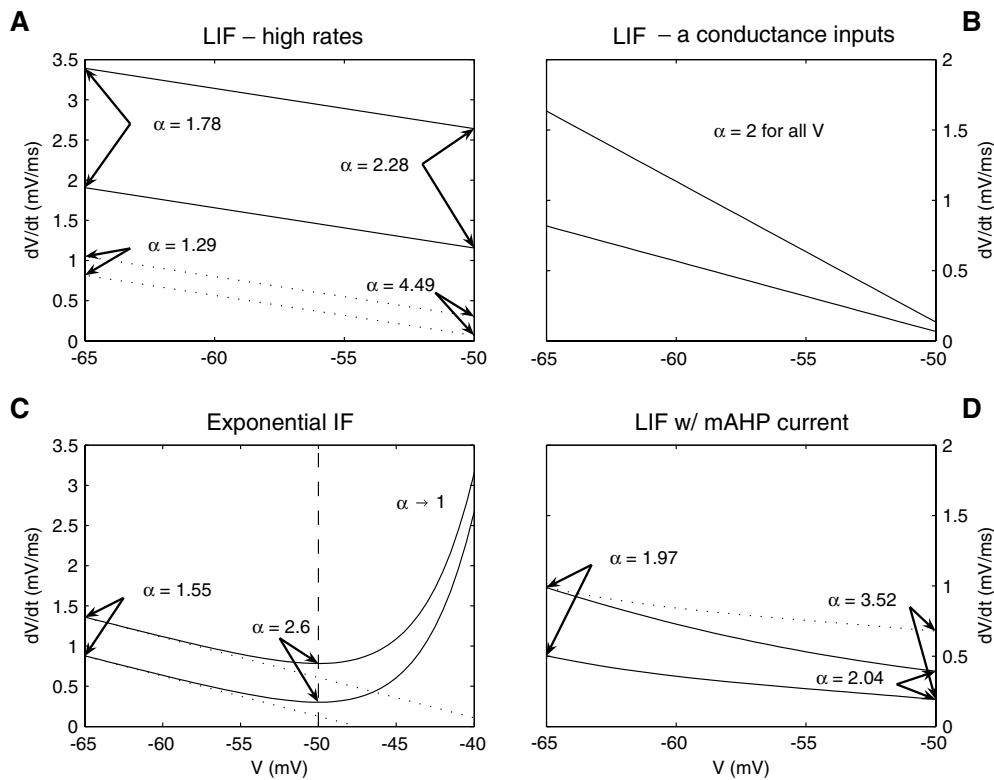


**Fig. 2** Summary of mechanisms affecting phase synchronization (see text for details). Voltage derivative is plotted as a function of voltage before (lower line) and after (upper line) a step increase in input. The ratio of voltage derivatives  $\alpha$  is shown for specific values of the voltage. (A) At high firing rates (transitions from 100 to 200 Hz; solid lines), the difference in leak current between reset and threshold voltages is less significant relative to the magnitude of the external current. Dotted lines: low rate transitions from 20 to 40 Hz. (B) A specific combination of input conductances causes a uniform multiplication of the voltage derivative, eliminating phase synchronization. (C) The depolarizing

current in the EIF model reduces the maximum value of  $\alpha$  by “speeding up” trajectories as they approach threshold (vertical dashed line; see section). During the spike, intrinsic currents dominate, yielding  $\alpha = 1$ . Dotted lines: derivatives with exponential current removed. (D) The addition of a potassium conductance “slows down” voltage trajectories after a spike, resulting in more uniform values of the voltage derivative. However, just after a transient the input current has increased, but the potassium current has not (dotted line), resulting in only a modest reduction in phase synchronization

baseline (Fig. 2A, solid lines). Therefore, vertically translating the line by changing  $I$  is roughly equivalent to scaling the derivative by a constant.

Synaptic conductances

An alternative to overpowering the intrinsic current term  $F(V)$  is to consider changes in input that increase the voltage derivative in a manner that is matched to the voltage dependence of  $F(V)$ . In particular, we will show that a LIF model receiving a particular step change in synaptic conductances can result in a transition in firing rates that induces no phase synchrony (Fig. 1, right). By adding excitatory and inhibitory conductances to the LIF equations we obtain

$$C \frac{dV}{dt} = g_l(V_{rest} - V) + g_e(V_e - V) + g_i(V_i - V) \quad (13)$$

where  $g_e$  and  $g_i$  are the level of excitatory and inhibitory conductances, with reversal potentials  $V_e$  and  $V_i$  respectively. If

we let  $G = g_l + g_e + g_i$  be the total membrane conductance, then we have

$$\begin{aligned} \tau \frac{dV}{dt} &= -V + (g_l V_{rest} + g_e V_e + g_i V_i) / G \\ &= -V + V^\infty \end{aligned} \quad (14)$$

where  $\tau = C/G$  is the membrane time constant and  $V^\infty$  is the equilibrium voltage in the absence of spiking. It follows that if changes are made in  $g_e$  and  $g_i$  that affect  $\tau$  but leave  $V^\infty$  unchanged, then we will achieve a multiplicative scaling of  $\frac{dV}{dt}$  at all voltages. The desynchronized voltage distribution will be identical before and after the change in input and no phase synchrony will be induced (Fig. 2B).<sup>2</sup>

<sup>2</sup> It is easy to show that the condition on the change in conductances  $\Delta g_e$  and  $\Delta g_i$  that guarantees  $V^\infty$  remain fixed is that the new conductances have a net reversal potential equal to  $V^\infty$ , i.e.  $(\Delta g_e V_e + \Delta g_i V_i) / (\Delta g_e + \Delta g_i) = V^\infty$ .

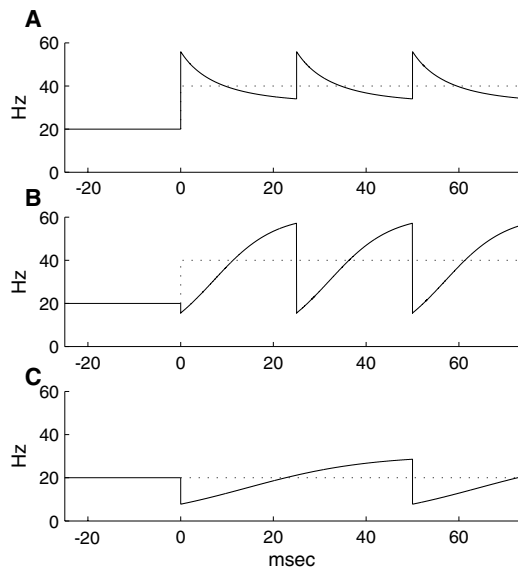


**Fig. 3** Different patterns of phase synchrony induced by changing input conductances. In all simulations, the pre-step parameters were: Rate = 20 Hz;  $\tau = 20$  msec;  $V^\infty = -48.66$  mV; exc. cond. = 0.0152 mS/cm<sup>2</sup>; inh. cond. = 0.0223 mS/cm<sup>2</sup>. The post-step parameters were: (A) Rate = 40 Hz;  $\tau = 12.49$  msec;  $V^\infty = -47.66$  mV; exc. cond. = 0.0256 mS/cm<sup>2</sup>; inh. cond. = 0.0420 mS/cm<sup>2</sup>. (B) Rate = 40 Hz;  $\tau = 20/6.57$  msec;  $V^\infty = -49.66$  mV; exc. cond. = 0.0442 mS/cm<sup>2</sup>; inh. cond. = 0.0955 mS/cm<sup>2</sup>. (C) Rate = 20 Hz;  $\tau = 13.14$  msec;  $V^\infty = -49.66$  mV; exc. cond. = 0.0221 mS/cm<sup>2</sup>; inh. cond. = 0.0415 mS/cm<sup>2</sup>. Leak cond. = 0.0125 mS/cm<sup>2</sup> for A–C and Fig. 1 (right)

If inputs are chosen that don't exactly match this criterion, phase synchrony will be reduced, but not eliminated. Interestingly, the shape of the post-transient pattern of firing rates will be reversed depending on whether the change in input increases or decreases the value of  $V^\infty$ . For input changes that increase overall firing rate and push  $V^\infty$  to more depolarized levels, the ensemble rates will resemble the pattern for an increase in current, but the modulation will be reduced (Fig. 3A). However, for input changes that increase overall firing rate yet decrease  $V^\infty$  to more hyperpolarized levels, the pattern of post-transient firing rates will be reversed with the peak rate occurring at the end rather than the beginning of the cycle (Fig. 3B). To increase rates while reducing  $V^\infty$  requires the input to contain a large fraction of inhibitory input so that increase in firing is due to a large increase in membrane conductance which substantially reduces the membrane time constant. It is also clear from this analysis that a transient change in input could change  $V^\infty$  and  $\tau$  in such a way that overall firing rate stays constant. Phase synchrony is still induced since these changes affect the shape of the equilibrium density (Fig. 3C).

#### Sodium currents

An alternative strategy for reducing phase synchronization is for the intrinsic current term  $F(V)$  to be relatively

constant over  $V$ . That way, a vertical translation of the  $\frac{dV}{dt}$  line will approximate a vertical scaling. One way to counteract the negative slope in  $F(V)$  contributed by the leak current is to speed up the voltage as it approaches threshold. Natural candidates for such a mechanism are fast sodium currents, either the non-inactivating “persistent” sodium current or the transient current that contributes to spiking.

A common method for simplifying the dynamics of such fast currents is to assume that the activation state of the current is an instantaneous function of the voltage  $\psi(V)$ , so that  $F(V) = g_l(V_{\text{rest}} - V) + \psi(V)$ . In a further simplification, Fourcaud-Trocme et al. (2003) have shown that near threshold,  $\psi(V)$  can be approximated by an exponential function, yielding the exponential integrate-and-fire (EIF) model. We will use  $\psi(V) = g_l \Delta_T \exp((V - V_T)/\Delta_T)$  with  $V_T = V_{\text{thresh}} = -50$  mV and  $\Delta_T = 3.5$  mV. The EIF model differs from the standard LIF in that it does not include a fixed voltage that acts as spike threshold. The definition of  $V_{\text{spike}}$  relies on the fact that as one follows the dynamics at more depolarized voltages, the exponential term comes to dominate and the voltage diverges to infinity in finite time. Setting  $V_{\text{spike}} = \infty$ , the EIF model can be viewed as setting the spike time at the peak of a spike. Note that  $\psi(V)$  is defined so that the minimum value of  $F(V)$  occurs at  $V = V_T$ . Therefore if one were start from rest and increase external current very slowly, the model will begin to fire when the current is sufficient to depolarize the cell to  $V_T$ . In this limited sense,  $V_T$  acts like a spike threshold.

Figure 4 shows results from an EIF model in response to a step change in input that increases ISI rate from 20 to 40 Hz. The shape of the post-transition modulations in PSTH-rate differs significantly from the LIF model. In particular, the rate rises continuously after the current step, starting from the pre-transition rate and then rising to a peak. After reaching the peak there is a slow decrease in rate, followed by a sharp dip back to the original firing rate at the end of each cycle. To understand this shape, we focus on the voltage  $V_T$ , where the voltage derivative reaches it's minimum. In analogy with the LIF model, trajectories in the EIF model accumulate near  $V_T$ , not the spike voltage  $V_{\text{spike}} = \infty$ . Thus, the peak firing rate comes from trajectories that were passing through  $V_T$  at the time of the input step. As a result, the peak occurs after a delay equal to the time it takes to travel from  $V_T$  to  $V_{\text{spike}}$ .

The continuous rise to the peak rate and the sharp transition at the end of each cycle result from the nature of the voltage dynamics just before and after a spike (Fig. 2C). As the voltage increases on its way to infinity, the exponential current comes to dominate and the ratio of voltage derivatives  $\alpha$  approaches one, no matter what the value of the external current. From Eq. (11), the post-step firing rate is equal to  $r_{\text{ISI}}^- \alpha(V_0(t))$ . Since the firing rate just after the step is determined by voltages reached just before a spike, the firing

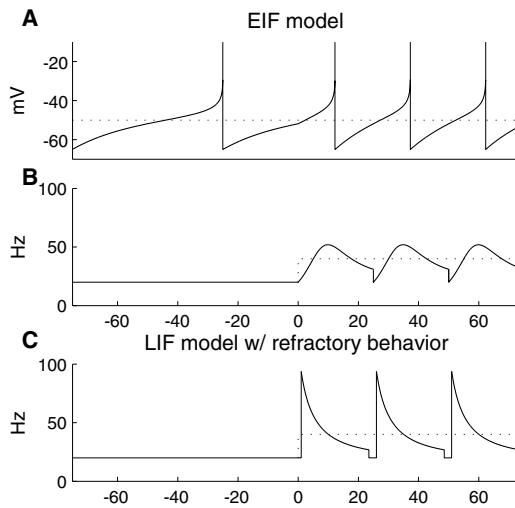


**Fig. 4** Phase synchronization in the EIF model and LIF model with refractory period. (A) Example voltage trace (EIF model). (B, C) Ensemble firing rate (B. EIF model; C. LIF model). Compare with Fig. 1

rate after the step is approximately equal to  $r_{ISI}^-$  and rates are continuous at  $t = 0$ . Moreover, because the pattern of firing rates is periodic, the firing rate shows a “dip” to the pre-step firing rate  $r_{ISI}^-$  at the beginning of each cycle. Note that the phenomenon of a dip in ensemble firing rate back to the pre-transition rate will be found in any model where (i) spiking dynamics play out over a finite period of time and (ii) spike shape is relatively invariant to changes in input. The apparent lack of a dip in the firing modulations in the LIF model is due the fact that spikes in this model are instantaneous. Figure 4C shows the firing rate modulations obtained from a LIF model with the same membrane parameters in Fig. 1 but where crossing threshold leads to an event in which the spike time is recorded 1.0 msec after crossing threshold, and voltage integration resumes at a hyperpolarized potential 1.5 msec later. Thus, inclusion of a slightly more realistic spike event to the LIF model restores two of the qualitative features of the post-transient response obtained from the EIF model: a delay between the time of the input transient to the peak firing rate and a dip in the rate back to the pre-transient firing rate at the end of each cycle. However, the sharp voltage threshold still manifests as an instantaneous increase in firing rate after the delay, as opposed to the more gradual increase from the EIF model.

#### After-spike potassium currents

We now return the focus to mechanisms that make the voltage derivative more uniform over subthreshold ranges of voltage. Our expectation was that slowing the voltage down as it leaves spike reset would have a similar effect as speeding up the voltage as it approaches threshold, and would also reduce the maximum firing rate after a step transient.

A candidate mechanism to cause such a slow down is the presence of potassium currents that linger after the spike. Action potentials activate a host of such currents, with activation time scales ranging from one or two milliseconds to several seconds. We focus here on currents that are slow enough to be active during a significant portion of an ISI, but are sufficiently fast to show significant decay from the beginning to the end of the ISI, such as the “mAHP” currents recorded in cortical and hippocampal neurons (e.g. Madison and Nicoll, 1984). In contrast to the fast sodium dynamics, these slower dynamics cannot easily be approximated as a function of voltage, requiring the consideration of a separate dynamic equation. Given these complications, we perform a rudimentary analysis within the framework of this paper, but do not pursue these models in detail. (For a more extensive exploration of related issues, see Gutkin et al., 2005.)

We consider a highly simplified two variable model, where the first variable is the voltage  $V(t)$  and the second variable is a spike-triggered potassium conductance  $u(t)$ . After each spike,  $u(t)$  is set to a fixed level  $u_{reset}$  and then it decays exponentially with a time constant of  $\tau_u = 35$  msec (Madison and Nicoll, 1984; see Methods). For a fixed input current  $I$ , trajectories will follow a fixed path ( $u(t), V(t)$ ). Along that trajectory we can consider  $u$  to be an implicit function of the voltage,  $u(V(t)) = u(t)$ , and calculate the voltage derivative as a function of  $V$  using Eq. (2). Following the analysis above, we can then calculate the voltage derivative ratio  $\alpha$  as a function of  $V$ . By choosing appropriate parameters for the potassium current ( $u_{reset} = 0.57$  g), the ratio  $\alpha$  can be made to be nearly constant (Fig. 2D). However, calculating phase synchrony using simulations of the original two-dimensional model yields a peak rate of 74.6 Hz (see Methods for details), only a slight reduction from that of the LIF model (89.9 Hz). The reason for this can be understood if we consider what happens to trajectories that are approaching threshold when the input is increased. The change in input takes effect immediately, whereas the potassium dynamics remains unchanged until the cell fires a spike. Therefore, to estimate the peak in ensemble firing rate after the transition, we should consider the voltage derivative calculated using Eq. (2) with the post-transition value for the external current  $I$ , but with the pre-transition function  $u(V)$  (Fig. 2D, dotted line). Indeed, the  $\alpha$  ratio from this calculation equals 3.52, which is in relatively good agreement with the corresponding ratio calculated from the simulated rates,  $74.6 \text{ Hz}/20 \text{ Hz} = 3.73$ .

#### Relationship to the phase response curve

Several of the results presented here can be obtained by an alternative derivations based on the phase response curve (PRC; Brown et al., 2004a; Gutkin et al., 2005). The PRC can

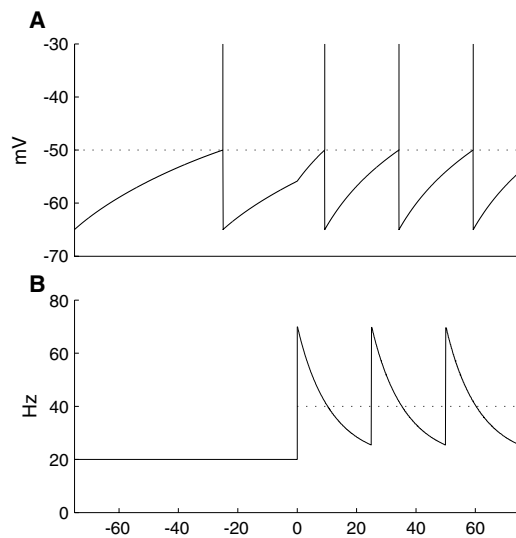


**Fig. 5** Phase synchrony in the LIF model with a spike-triggered potassium conductance. (A) Example voltage trace. (B) Ensemble firing rate

be understood as the result of the following experiment. Suppose a neuron receives a constant level of current sufficient to cause a steady rate of firing. In addition to this constant current, small pulses of current are sporadically injected at different phases of the oscillation and the change in time  $\Delta t$  of the next spike relative to the base period is recorded. By convention, speeding up of spiking is usually assigned a positive value of  $\Delta t$ . A plot of how  $\Delta t$  depends on the phase of the oscillation at which the pulse is delivered is proportional to the PRC.

Translating this experiment to the generalized IF model in Eq. (1), we note that each pulse of current results in a small instantaneous depolarization of fixed magnitude  $\Delta V$ . The time to the next spike will be shortened by the time it normally takes to travel a distance  $\Delta V$  along the trajectory, or  $\Delta V / \frac{dV}{dt}$ . Therefore, both the PRC and the equilibrium density  $\tilde{\rho}(V)$  are inversely proportional to the derivative of the voltage. So for generalized IF models with no noise, *the desynchronized density is equivalent to the PRC, the only difference being that the density is viewed as a function of voltage and the PRC is viewed as a function of phase.*

## Discussion

We have employed a probability density approach to understand the mechanisms contributing to phase synchronization in a class of generalized integrate-and-fire neurons subject to a step change in input. For the noiseless case, the time-course of post-transient ensemble firing rate depends on the ratio  $\alpha(V)$  which measures the ratio of the voltage derivative before and after the change in input. In

particular, step inputs induce phase synchrony to the degree that the ratio of derivatives  $\alpha(V)$  is non-uniform across voltage. Because it is relatively easy to determine how various biological mechanisms affect the voltage derivative, this approach helps to clarify the range of factors contributing to transient-induced synchronization in these networks.

## Subthreshold factors affecting synchronization

This paper considered four factors affecting phase synchronization. We focus here on subthreshold integration. A discussion of spiking follows in the next section.

The first factor considered is the magnitude of the external input current. When the input current is sufficiently large it dominates the voltage-dependent intrinsic currents. As a result, changes in the voltage derivative are relatively uniform across all voltages and these inputs induce a relatively small degree of phase synchrony.

Second, we examined rate changes induced by a step change in excitatory and inhibitory conductance. Such input changes affect spike rate by two separate mechanisms: by changing the membrane time constant and/or by changing the combined synaptic and intrinsic reversal potential,  $V^\infty$ . Inputs that only change the membrane time constant result in a uniform scaling of the voltage derivative and hence induce zero phase synchrony. For inputs that change the net reversal potential, the shift in this potential determines the relative timing of the increases and decreases in post-transient firing rate. If  $V^\infty$  shifts closer to threshold and yet firing rates increase, the pattern of phase synchrony will be opposite to that induced by shifting  $V^\infty$  to more depolarized levels (Fig. 3). These results highlight the fact that the relative balance of excitation and inhibition has a strong influence on the shape of the equilibrium distribution for fixed levels of input, and hence will also have a strong influence on the synchronization properties of neurons subject to changing inputs.

Third, we looked at the influence of fast sodium currents by examining phase synchrony in the exponential integrate-and-fire (EIF) model. These currents served to increase the voltage derivative as trajectories approached the threshold voltage, thus partially counter-acting the buildup of trajectories near threshold seen in the LIF model. As a result, the peak firing rate after a step increase in current was reduced for the EIF model relative to the LIF model.

Finally, we considered the effect of adding spike-triggered potassium currents to the LIF model. By slowing down the voltage derivative after a spike, it was expected that these currents would reduce phase synchronization by making the voltage derivative more uniform as a function of voltage.

However, implementing these currents in an extended LIF model led to only a slight reduction in phase synchronization. The underlying reason is that changes in input current affect the voltage dynamics instantly, but potassium currents remain unaffected until after the next spike. It is unclear how this temporal mismatch may affect the dynamics for more complex situations than those studied here (e.g. see Gutkin et al., 2005).

#### Separating “integrate” from “fire”

A defining feature of the IF class of models is the use of voltage thresholds and voltage reset to separate the “integrate” from the “fire.” In particular, these mechanisms serve as simplified substitutes for the dynamics underlying the initiation and/or termination of action potentials. In relation to the analysis presented here, voltage reset introduces a discontinuity in the voltage derivative along trajectories which lead to sharp transitions in the post-step ensemble firing rate.

In the standard LIF model, subthreshold intrinsic currents are a simple linear function of voltage and spikes are instantaneous events triggered at a fixed voltage threshold. However, over the past decade, the notion of spike threshold has come under closer scrutiny. A commonly exploited analytical approach is the use of bifurcation theory to examine the loss of stability near the onset of spiking. The resulting normal form equations can be used as simplified neuron models that take into account the effect of voltage dependent intrinsic currents (e.g. Brown et al., 2004a; Ermentrout, 1996; Ermentrout and Kopell, 1986; Hoppensteadt and Izhikevich, 1997; Latham et al., 2000). The strict applicability of these equations holds only in the limit of very low rates where the temporal behavior of the model is dominated by the dynamics of trajectories near the bifurcation. Like the LIF models, spikes are relegated to a fast event that separates periods of voltage integration. However, many neurons fire at rates where the strong spiking currents are likely to be important during a significant portion of an interspike interval and may play an important role in determining a neuron’s reaction to changes in external input (e.g. Figs. 4B and C). For example, a 2.5 msec spiking event takes up 10% of the period for a neuron firing at 40 Hz.

The EIF model (Fourcaud-Trocme et al., 2003) can be seen as an attempt to more realistically model the transition from integration to spiking within the context of the one-dimensional IF framework. The transition from spiking back to integrating is still handled using a threshold and reset mechanism. Given that the mechanisms contributing spike repolarization are slow relative to the voltage dynamics, constructing ensemble dynamics that more realistically model the transitions between integrating and firing in *both* directions may require the extension of population

density techniques to two-dimensional dynamic models (see Gerstner and Kistler, 2002) for references to classical 2D models; see Izhikevich, 2003 for a simple 2D IF-like model).

#### Relation to phase methods

When studying the factors affecting synchrony within ensembles of neural oscillators, it is common to separate issues of phase and frequency by studying perturbations around a fixed base frequency (e.g. Brown et al., 2004a; Ermentrout 1996; Gutkin et al., 2005; Hansel et al., 1995; Hoppensteadt and Izhikevich, 1997 and references therein). By changing variables, one is often able to write the dynamics as  $d\theta/dt = \omega + \epsilon f(\theta)$  where  $\theta$  is the phase of the unperturbed system,  $\omega$  its angular velocity, and  $\epsilon f(\theta)$  represents a small perturbation. Although this approach simplifies many types of analysis, the underlying biological parameters can get obscured during the change of variables. Moreover, because a different change of variables is generally needed for each base frequency, it can be difficult to understand system behavior over a range of frequencies. The approach taken in this paper has the advantage of relying on a single, biologically interpretable coordinate system. This perspective makes it clear that phase synchronization depends on the relative magnitude of the distribution of states driven by past input and the equilibrium distribution corresponding to the current level of input. Moreover, because the state space is readily interpretable, understanding how physiologically relevant changes will affect the dynamics is relatively straightforward.

A key element of many phase-based analyses is the phase response curve or PRC, representing how a perturbation at a given point in time affects the time of the next spike. From the perspective of a fixed underlying coordinate system, there are two separable factors that contribute to the PRC. First, one must determine how sensitive the underlying state is to perturbations at various points along the limit cycle. Second, one must determine how that state perturbation is translated into a perturbation in time. For the class of models analyzed in this paper, calculating both factors is straightforward. A small perturbing current moves the voltage by a fixed amount, and the effect of that perturbation on the time of the next spike is inversely proportional to the voltage derivative at that point. Given that the first factor is not state dependent and that the equilibrium density is also inversely proportional to the voltage derivative, in these models the PRC and the equilibrium density are proportional. In more general models, two factors may intervene to cause the PRC and equilibrium density to differ. First, the addition of noise will add a diffusive component to the equilibrium density and will complicate the relationship between the density and

voltage derivative. Second, the magnitude of perturbations in the underlying state space may be state dependent.

#### Limitations and extensions

The analysis presented here relies heavily on using membrane voltage as a fixed coordinate system to analyze the dynamics across levels of external input. In generalized IF oscillators a fixed state space is guaranteed by the reset mechanism that returns the voltage to the same value after each spike. However, voltage reset is simply a convenient simplification and masks a range of dynamic phenomena that contribute to the hyperpolarization ending a spike and the voltage integration that follows. Since many of these mechanisms are likely to be affected by the level of external input, extending the approach taken in this paper to more realistic models will require an examination of how the changes in external input affect the structure of the underlying state space.

To facilitate our analysis, we have assumed piece-wise constant inputs and no noise. This “freezes” the effect of a step change in input into a pattern of phase synchrony that persists indefinitely in time. The consideration of noisy, time-varying inputs introduces a number of complications. However, our analysis suggests one possible approach: view the ensemble density at a given time as the product of the equilibrium density for the current input and a phase-synchrony ratio  $\alpha(V)$  representing the relative magnitude of the actual and equilibrium densities. Given this parsing of the probability density, the full dynamics of the system is governed by three basic mechanisms. First, changes in the input will result in a multiplication of the  $\alpha$  ratio by a factor that depends on the change in the equilibrium distributions that correspond to the changing input. This is the “engine” that drives phase synchronization. Second, the  $\alpha$  ratio will be subject to the underlying oscillatory dynamics in the system and will “follow” trajectories of the system, i.e. with constant input and no noise,  $\alpha(V(t)) = \alpha(V(t'))$  where  $V(t)$  and  $V(t')$  lie along a single trajectory. Finally, noise introduced into the system adds a diffusive component to the  $\alpha$  ratio, so that  $\alpha$  has a tendency to decay toward a uniform value of one, reducing phase synchrony in the system (Knight, 1972). It is the interaction between these factors that will determine the dynamic response of the system to complex inputs.

**Acknowledgments** I thank Joanna Pressley for useful discussions, and Jason Ritt for comments on a draft of this manuscript. I gratefully acknowledge support from a Sloan Research Fellowship.

#### References

- Amari S (1974) A method of statistical neurodynamics. *Kybernetik* 14(4): 201–215.
- Brown E, Moehlis J, Holmes P (2004a) On the phase reduction and response dynamics of neural oscillator populations. *Neural Comput.* 16(4): 673–715.
- Brown E, Moehlis J, Holmes P, Clayton E, Rajkowski J, Aston-Jones G (2004b) The influence of spike rate and stimulus duration on noradrenergic neurons. *J. Comput. Neurosci.* 17(1): 13–29.
- Brunel N (2000) Dynamics of sparsely connected networks of excitatory and inhibitory spiking neurons. *J. Comput. Neurosci.* 8(3): 183–208.
- Ermentrout B (1996) Type I membranes, phase resetting curves, and synchrony. *Neural Comput.* 8(5): 979–1001.
- Ermentrout B, Kopell N (1986) Symmetry and phaselocking in chains of weakly coupled oscillators. *Comm. Pure Appl. Math.* 39(5): 623–660.
- Fourcaud-Trocme N, Brunel N (2005) Dynamics of the instantaneous firing rate in response to changes in input statistics. *J. Comput. Neurosci.* 18(3): 311–321.
- Fourcaud-Trocme N, Hansel D, van Vreeswijk C, Brunel N (2003) How spike generation mechanisms determine the neuronal response to fluctuating inputs. *J. Neurosci.* 23(37): 11628–11640.
- Gerstner W (2000) Population dynamics of spiking neurons: Fast transients, asynchronous states, and locking. *Neural Comput.* 12(1): 43–89.
- Gerstner W, Kistler W (2002) *Spiking Neuron Models*. Cambridge Univ. Press, Cambridge, UK.
- Gutkin B, Ermentrout G, Reyes A (2005) Phase-response curves give the responses of neurons to transient inputs. *J. Neurophysiol.* 94: 1623–1635.
- Hansel D, Mato G, Meunier C (1995) Synchrony in excitatory neural networks. *Neural Comput.* 7(2): 307–337.
- Hermann A, Gerstner W (2001) Noise and the PSTH response to current transients: I. General theory and application to the integrate-and-fire neuron. *J. Comput. Neurosci.* 11(2): 135–151.
- Hoppensteadt F, Izhikevich E (1997) *Weakly Connected Neural Networks*. Springer, New York.
- Izhikevich E (2003) Simple model of spiking neurons. *IEEE Trans. Neural Networks* 14: 1569–1572.
- Knight B (1972) Dynamics of encoding in a population of neurons. *J. Gen. Physiol.* 59(6): 734–766.
- Knight B, A. O, Sirovich L (2000) The approach of a neuron population firing rate to a new equilibrium: An exact theoretical result. *Neural Comput.* 12(5): 1045–1055.
- Latham P, Richmond B, Nelson P, Nirenberg S (2000) Intrinsic dynamics in neuronal networks. I. Theory. *J. Neurophysiol.* 83: 808–827.
- Madison D, Nicoll R (1984) Control of the repetitive discharge of rat CA1 pyramidal neurones in vitro. *J. Physiol.* 354: 319–331.
- Moreno-Bote R, Parga N (2005) Membrane potential and response properties of populations of cortical neurons in the high conductance state. *Phys. Rev. Lett.* 94: 088103.
- Naundorf B, Geisel T, Wolf F (2005) Action potential onset dynamics and the response speed of neuronal populations. *J. Comput. Neurosci.* 18(3): 297–309.
- Nykamp D, Tranchina D (2000) A population density approach that facilitates large-scale modeling of neural networks: Analysis and an application to orientation tuning. *J. Comput. Neurosci.* 8(1): 19–50.
- Omurtag A, Knight B, Sirovich L (2000) On the simulation of large populations of neurons. *J. Comput. Neurosci.* 8(1): 51–63.
- Riccardi L (1977) *Diffusion Processes and Related Topics in Biology*. Springer-Verlag.
- Salinas E, Sejnowski T (2001) Correlated neuronal activity and the flow of neural information. *Nat. Rev. Neurosci.* 2(8): 539–550.
- Stein R (1965) A theoretical analysis of neuronal variability. *Biophys. J.* 91: 173–94.
- Wilson H, Cowan J (1972) Excitatory and inhibitory interactions in localized populations of model neurons. *Biophys. J.* 12(1): 1–24.